MESH–WRAP RETROFITTING FOR RAMMED EARTH BUILDINGS – TEST RESULTS OF FULL–SCALE STATIC TESTS

P. Wangmo[1], K.C. Shrestha [2], T. Aoki[3], M. Miyamoto[4], N. Takahashi[5], J. Zhang[6], N. Yuasa[7], S. Shin[8], Pema[9], F. De Filippi[10], R. Pennacchio[11]

[1] *Engineer, Department of Culture, Ministry of Home and Cultural Affairs, pwangmo@mohca.gov.bt*
[2] *Assistant Professor, Graduate School of Design and Architecture, Nagoya City University, kshitij@sda.nagoya-cu.ac.jp*
[3] *Professor, Graduate School of Design and Architecture, Nagoya City University, aoki@sda.nagoya-cu.ac.jp*
[4] *Associate Professor, Faculty of Engineering and Design, Kagawa University, miyamoto@eng.kagawa-u.ac.jp*
[5] *Associate Professor, Graduate School of Engineering, Tohoku University, ntaka@archi.tohoku.ac.jp*
[6] *Associate Professor, Graduate School of Engineering, Kyoto University, zhang@archi.kyoto-u.ac.jp*
[7] *Professor, Department of Architecture and Architectural Engineering, Nihon University, yuasa.noboru@nihon-u.ac.jp*
[8] *Postdoctoral fellow, Department of Architecture and Architectural Engineering, Nihon University, shin.sangchul@nihon-u.ac.jp*
[9] *Deputy Executive Engineer, Department of Culture, Ministry of Home and Cultural Affairs, pema_engineer@mohca.gov.bt*
[10] *Associate Professor, Department of Architecture and Design, Politecnico di Torino, francesca.defilippi@polito.it*
[11] *Research Fellow, Department of Architecture and Design, Politecnico di Torino, roberto.pennacchio@polito.it*

Abstract

The rural houses in the western region of Bhutan are predominantly constructed using rammed earth material, which constitute more than 70% of present residential houses and are also preserved as traditional buildings. Unfortunately, these buildings suffered significant destruction by the 2011 Sikkim earthquake with a magnitude of 6.9. This work proposes a practically feasible and effective mesh–wrap retrofitting solution, to improve the seismic performance of these traditional Bhutanese rammed earth buildings. The effectiveness is verified through full–scale static tests. For this purpose, two 2–storied full–scale rammed earth buildings were tested in December 2018. Tested buildings represent the typical rammed earth houses in Bhutan, incorporated with traditional architecture design without any seismic resilient features. The same set of buildings were later retrofitted (after the first phase of testing) with mesh and braces in the floor joists. The first phase of full–scale test was conducted on unreinforced rammed earth buildings at two different orientations to study the effect of building's asymmetry towards the structure's global response, both to short–span (RE–U-SHORT), and long–span (RE–U-LONG) loading. Afterwards, the full–scale static test second phase was conducted on the retrofitted buildings (RE-R–SHORT and RE–R-LONG) in March 2019. The resulting damages in the buildings were documented through visual observation after every test runs for specific story-drift. The test results showed the load carrying capacities were improved substantially with the mesh–wrap retrofitting technique by 2.43 times and 3.25 times for short–span and long–span loaded buildings, respectively. The proposed retrofitting technique was also found effective in improving the energy absorption and ductility index.

Keywords: Rammed earth; full–scale static test; building orientation; retrofitting; Bhutan

1. Introduction

In the last few decades, the earthquakes around the world have highlighted the vulnerability of rammed earth structures [1,2,3,4] due to their brittle behavior particularly when lacking of effective seismic resistant design. Bhutan has a rich repository of rammed earth construction ranging from historical monuments to the residential buildings. In particular, rural houses in the western region of Bhutan are predominantly rammed earth preserved as traditional buildings, and constitute more than 70% of present residential houses. Unfortunately, these buildings suffered significant destruction by the 2011 Sikkim earthquake (M6.9) that occurred between the Nepal-India border [1,5]. Fig. 1 shows some of the failures observed in rammed earth buildings affected [6]. Few studies have been carried out on retrofitting measures to improve the seismic performance of existing rammed earth structure by using canvas, bamboo and tarpaulin as externally bonded fibers with different adhesive materials [2] and tarpaulin [3], steel plates configured in a grid system on both faces of the wall [4] flax–fiber reinforcement [7], polyester fabric strips [8] and jute fabric [9] and cement mortar–steel fiber reinforcement [10]. However, all these studies were realized on a small-scale element test and some of the proposed retrofitting techniques can be restricted on real field due to high cost and complicated process involved. Current study proposes a simple, feasible and cost-effective retrofitting technique. Furthermore, it is the first full-scale test conducted on prototype rammed earth buildings to check the building response at two different orientations, while investigating the strengthening effect of mesh-wrap retrofitting technique, to improve the seismic performance of these traditional Bhutanese rammed earth buildings.

(a) (b) (c) (d)

Fig. 1 – Rammed earth buildings damaged by 2011 earthquake: (a) Out-of-plane wall collapse; (b) Corner overturning; (c) Corner crack; (d) Vertical crack under loading point of floor joist.

2. Experimental program

2.1 Test specimen

Initially, two full-scale unreinforced buildings were constructed for static test at two different loadings, one loaded in short-span (RE-SHORT) and other in long-span (RE-LONG). The construction lasted almost four months and completed in early September 2018. The overview of full-scale static test is given in Fig.2. The specimens were the replication of the Bhutanese rammed earth building dominating typology having two stories, where the ground floor has solid walls with small openings for doors and windows, and the first floor has a large opening in the front façade. The design and dimensions for both rammed earth buildings were considered the same with a floor area of 8.1 m × 5.4 m and 6.83 m height excluding the roof (Fig.2). The building specimens were constructed over the strong reinforced concrete slab by local artisans, following the typical Bhutanese rammed earth construction practice [5,11,12]. The soil was prepared in order to get a suitable mixture by checking the correct water content through a traditional field test. A handful of moist earth is squeezed and tossed up in the air, about a meter away from the ground, the mixture is considered suitable if falling back on the ground, breaks into two or three major pieces [11]. About 200mm thickness moistened soil layer was then poured inside the wooden formwork (Fig.3) and rammed manually till the desired height, using

2

hardwood rammers having different base shapes. A rammer with hammer head was used for normal compaction and smooth finishing at the edges was achieved using a rammer with wedge head. The details of ramming tools used for compacting rammed earth layers are shown in Fig. 3. One completed rammed earth block consisted 600mm height and 600mm thickness, and the length of each block differed depending on the location of the openings. Each block comprised six rammed earth layers whose thickness was 100mm at its final compaction. The blocks at the corners (marked 1, 2 & 3 in Fig.3) and junctions are placed alternately to avoid continuous head joint.

Two parameters were considered for the current study, first the loading direction to the wall and second the retrofitting technique. The specimens were named according to the parameters: i) Rammed earth-unreinforced and loaded in short-span (RE-U-SHORT), ii) Rammed earth–retrofitted and loaded in short-span (RE-R-SHORT), iii) Rammed earth-unreinforced and loaded in long-span (RE-U-LONG) and iv) Rammed earth-retrofitted and loaded in long-span (RE-R-LONG). It should be noted that the RE-U-SHORT and RE-U-LONG were retrofitted after first phase of testing and they were renamed RE-R-SHORT and RE-R-LONG, respectively.
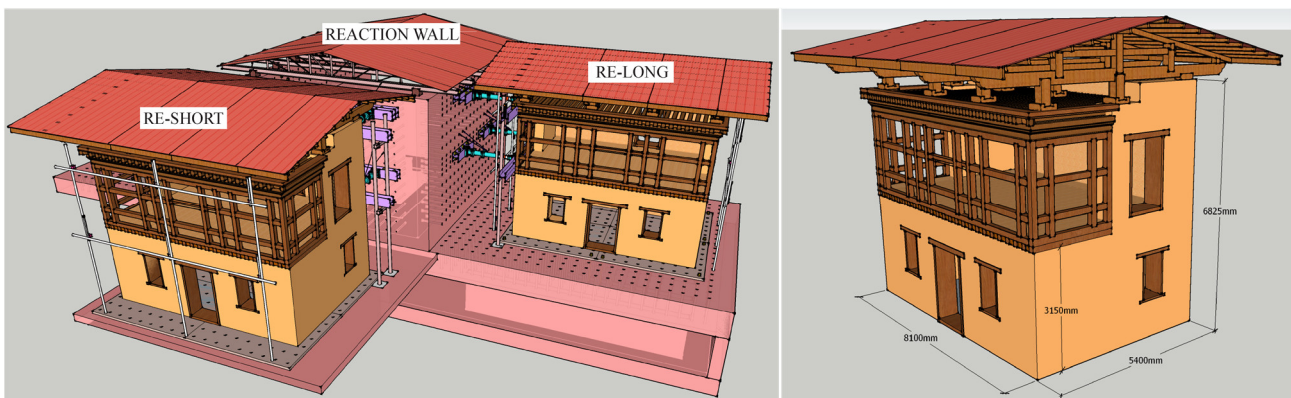

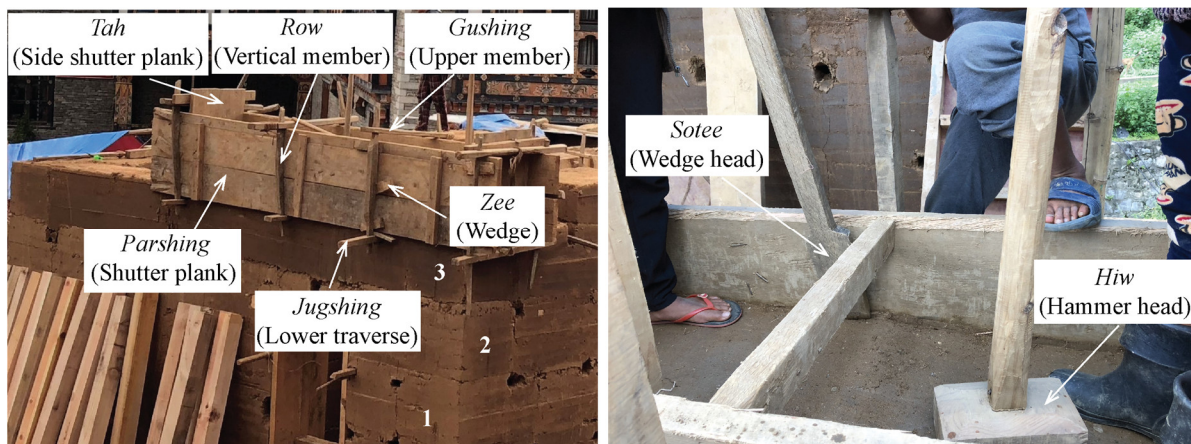Fig. 2 – Overview of full-scale static tests and specimen details

Fig. 3 – Formwork and ramming tools details

2.2 Retrofitting and bonding materials

2.2.1 Mesh

Two types of meshes with different sizes were selected, based on their availability in the local market, to retrofit the existing unreinforced rammed earth buildings. One of the meshes had 1.8mm diameter and 34x34

mm^2 opening. It served as the main mesh (M-mesh), provided in the entire wall from both inside and outside. Due to its size limitation, lapping was unavoidable. Thus, another more flexible mesh, easier to bend, was provided as a lapping mesh (L-mesh) over the M-mesh at their joints, corners and junctions. L-mesh comprised 1.45mm diameter and an opening of 28x28 mm^2.

2.2.2 Fastener

Fasteners were used to affix the meshes to the walls. U-hooks were used all through the wall to anchor mesh to the wall. Meshes on two faces of the wall were firmly connected by transversal threaded bars having 12mm diameter and 600mm length. These threaded bars were inserted through the *jugshing* holes, an opening created upon removal of *jugshing* (Fig. 3).

2.2.3 Cement mortar

Two governing criteria were considered on selection of mortar: (1) availability in the local market and (2) affordability. Based on these guidelines, cement mortar with cement and sand ratio of 1:3 was chosen. Cement mortar was applied over the mesh to provide good bonding between the wall and the mesh. The cement plaster also enhanced the aesthetic view of the wall surface with smooth finishing.

2.3 Retrofitting procedures

Immediately after the first phase of testing the unreinforced buildings RE-U-SHORT and RE-U-LONG, the retrofitting works were carried out in late December 2018, and they were renamed RE-R-SHORT and RE-R-LONG, respectively. A practically feasible and effective mesh-wrap retrofitting technique was considered for this study based on the material available in the local market. The retrofitting method was kept simple so that any local artisans can construct it without expert guidance, and the retrofitting cost was within 20% of the building cost. The mesh-wrap retrofitting technique was provided only for the in-plane walls in both faces of the walls. The step by step procedures for retrofitting work carried out is presented below:

(i) Fix M-mesh (highlighted with green in Fig. 4) on both faces of the wall using fasteners. The details of the mesh layout at the exterior face of the wall are presented in Fig.5, and it should be noted that the layout is maintained same in the interior face of the walls as well; The mesh was also provided at the floor levels of an elevation at which the loading was applied.

(ii) Lay L-mesh (highlighted with pink in Fig. 4) over the joints of M-mesh both in horizontal and vertical to avoid local failure of main mesh;

(iii) Provide uniform lapping length of 300mm in vertical and 60mm in horizontal;

(iv) Connect two meshes at interior and exterior of the wall by threaded bars;

(v) Apply cement slurry to wet the wall surface and prepare for plaster;

(vi) Apply first layer of cement plaster;

(vii) Apply second layer of plater to provide smooth finishing. The total thickness of the cement plaster provided is 30mm;

(viii) Provide timber bracing under the floor joists.

The entire retrofitting work for both the buildings were completed within three weeks. The specimens RE-R-SHORT and RE-R-LONG were tested again in March 2019 after two months of curing period. Some details of retrofitting work are presented in Fig. 5.
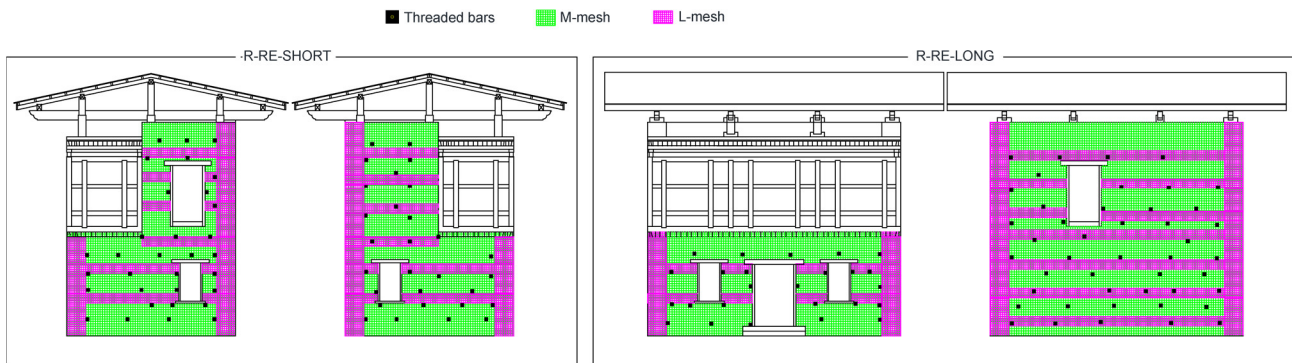
4

Fig. 4 – Mesh layout for rammed earth buildings (RE-R-SHORT and RE-R-LONG)

Fig. 5 – Retrofitting work details: (a) Fixing mesh; (b) Wetting wall surface with cement slurry; (c) Applying cement plaster; (d) Providing bracing under floor joists; (e) Final view of building after retrofitting work.

2.4 Test set up

The test setup and instrumentations for specimen loaded in short-span (RE-SHORT) and in long-span (RE-LONG) are illustrated in Fig. 6. Four static jacks were placed: two with 500kN capacity in first floor (1FL) and other two with 1000kN capacity at the second floor (2FL) to apply horizontal load at respective floors. One end of static jack was connected to reaction wall and other end to building specimen through H-section. The static jacks were operated manually with the hydraulic pumps to apply and release load. The setup helps to transfer uniform load to all the walls, and the distribution of load in each wall is assumed to be based on their respective stiffness. Each floor level of the building was subjected to displacement controlled loading to a specified target story-drift. The load applied in 1FL and 2FL were controlled to have the same story-drift during the loading process. Here, the story-drift is defined as the ratio of the lateral displacement to the floor height. Cracks and damage observed were documented at the story-drift: 0.05%, 0.1%, 0.13%, 0.2% for unreinforced rammed earth specimens. For retrofitted buildings, in addition to above drift values, the buildings were subjected to story-drift of 0.4%, 0.67%, 1.0% and 1.13%. The horizontal displacements during loading were recorded by 14 displacement transducers; 10 laser transducers and 4 linear variable displacement transducers (LVDTs) at three different levels of the test specimen placed both at the loading and the free side. A multi-channel dynamic strain meter DS-50A is used for data logging with LAN interface setting.
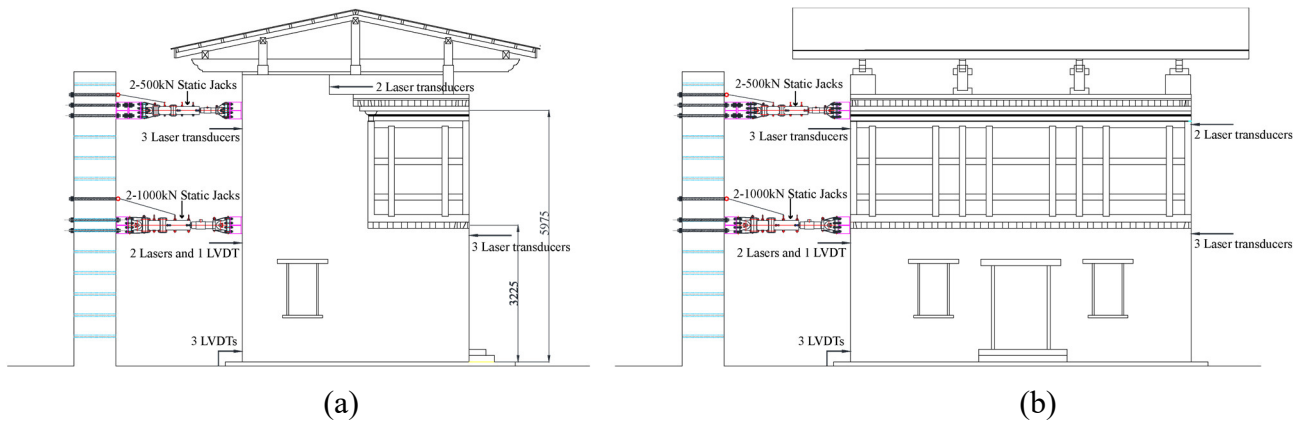
5

(a)   (b)

Fig. 6 – Full-scale static test set-ups: (a) Loaded in short-span, (b) Loaded in long–span.

2.5 Material test results

For the material test, cylindrical rammed earth specimens were extracted with a core drilling machine from each building specimens following the full-scale static test. The compressive and splitting tensile test were conducted according to the ASTM C39 [13] and ASTM C496 [14], respectively. The test results from the material test are summarized in Table 1.

Table 1 – Material characteristics for the tested samples

Specimen ID	RE-SHORT				RE-LONG			
Unit	ρ_b (kg/m³)	f_c (MPa)	f_t (MPa)	E	ρ_b (kg/m³)	f_c (MPa)	f_t (MPa)	E
Average	1836.7	0.94	0.12	248.89	2023.7	1.65	0.17	388.59
Standard dev.	32.9	0.12	0.02	57.86	12.92	0.15	0.03	55.19

ρ_b – Bulk density; f_c – Compressive strength; f_t – Tensile strength; E – Young's modulus

3. Results and discussion

3.1 Capacity curve and crack observations

The capacity curves for all tested specimens are presented in Fig. 7. The strength of the rammed earth building is represented in story shear, and the deformation is represented in terms of roof displacement and the top story-drift. Further, an equivalent base shear coefficient is also presented, given by the ratio of the cumulative base shear of the building (V_b) to the total seismic weight of the building (W_t = 1333 kN). The story shear at 1FL, which also represents the cumulative base shear, is taken as the summation of horizontal loads at 2FL and 1FL. To plot the top story-drift, the mean value of three transducers placed at 2FL are considered. The cumulative base shear from the experimental results of each building specimens is presented in Table 2. In both the loading cases, the specimens retrofitted with mesh showed better strength than their counterparts. The capacity of unreinforced building loaded in short-span (RE-U-SHORT) was improved by 2.43 times with the mesh-wrap retrofitting technique and for the unreinforced building loaded in long-span (RE-U-LONG) was improved by 3.25 times.

The capacity curve was almost linear when the story-drift was within 0.05% for RE-U-SHORT and RE-U-LONG, 0.13% for RE-R-SHORT and 1.0% for RE-R-LONG. On further application of the load, the response of rammed earth building specimens showed non-linear which was characterized by its first appearance of cracks. The damages for all the specimens were monitored at the predefined target story-drift through visual observations and video recordings. The resulting cracks are illustrated in Fig. 8 and Fig. 9 for the unreinforced and retrofitted buildings, respectively. Cracks for only in-plane walls are presented since the out-of-plane wall did not show major crack during the test. In general, the cracks evolved near the openings, loading areas and corners for the unreinforced buildings. For the retrofitted buildings, the cracks were usually
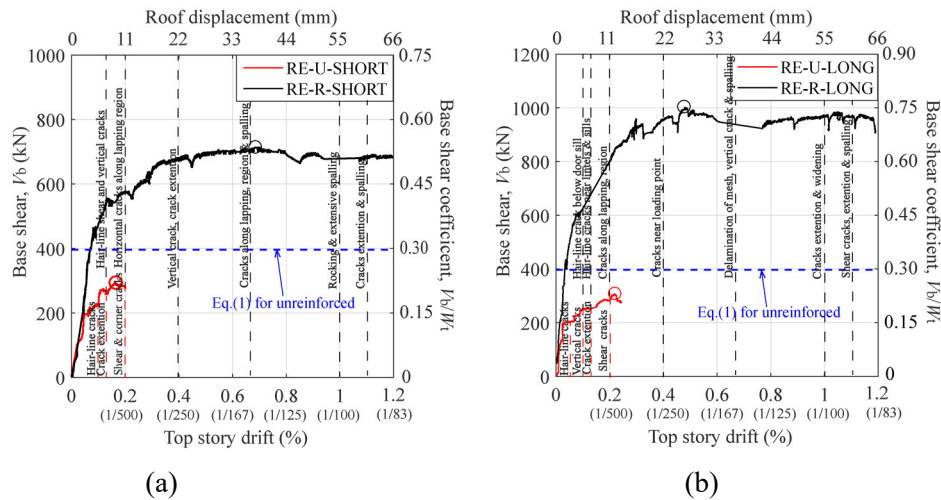
6

Fig. 7 – Relationship between base shear and story-drift: (a) Loaded in short-span and (b) Loaded in long-span

found in the lapping region of the mesh both in horizontal and vertical. The shrinkage cracks appeared during the drying period of the buildings are marked with black in Fig. 8 for the unreinforced buildings. These shrinkage cracks were normally found originating from the head joints, bed joints and near openings illustrating the vulnerable areas of rammed earth structures. The cracking evolution in each building are highlighted below:

RE-U-SHORT: No cracks were visible during the first stage of loading within story-drift of 0.05%. The first few hair-line cracks originated near openings, window sill, loading area and at top rammed earth block in east elevation, and near lintel and *jugshing* holes of west elevation when the story-drift was up to 0.1%. The cracks propagated on both in-plane walls on further application of load, and the story-drift was up to 0.13%. Within the story-drift of 0.2%, there was an extension of previous cracks and new shear crack in east elevation was also observed. In the west elevation wall, a vertical corner crack evolved 600mm away from the corner at the same story-drift. The test was stopped at story-drift of 0.2%.

RE-U-LONG: Few hair-line shear cracks were observed mainly originating near *jugshing* holes for both in-plane walls during the first phase of loading within story-drift of 0.05%. At story-drift of 0.1%, a horizontal crack propagated towards the window lintel in south wall along with minor cracks in other areas. In the north elevation, the existing long vertical crack (formed during the drying period) widened which could have been induced by an inside transverse wall perpendicular to this crack. At story-drift of 0.13%, few new minor cracks appeared both in in-plane walls. With the last phase of loading at story-drift of 0.2%, numerous shear cracks initiated in the north wall. In the south wall, a minor shear crack appeared above the door lintel.

RE-R-SHORT: No cracks were detected during the first and second phase of loading. However, in the third stage within the story-drift of 0.13%, cracks in lintels of both in-plane walls were noticed. There were also numerous vertical cracks between the two window openings of the west elevation. On further application of load within story-drift of 0.2%, the previous crack extended and horizontal crack initiated along the lapping areas in the west elevation. In east elevation, a vertical crack appeared along the lapping in the corner. When the story-drift was within 0.4%, a horizontal crack evolved near window of east elevation and corner crack in the top most rammed earth block. In west elevation, a long vertical crack appeared along the lapping region. Significant cracks were seen within the story-drift of 0.67%. The plaster started falling off as the crack extended. The building started rocking with the appearance of the crack in the base when the story-drift was within 1.0%. A crackling sound due to dislocation of timber components was heard on further application of load and the test had to be stopped at story-drift of 1.33 for safety reasons. Within story-drift of 1.33%, the previous crack propagated in size and there was extensive spalling of plaster.

7

<u>RE-R-LONG:</u> In the first stage of loading within the story-drift of 0.05%, cracks were invisible. In the next loading, a minor crack evolved near the sill level of door in south elevation within the story-drift of 0.1%. Few new minor cracks were visible near lintels and sills of both in-plane walls within the story-drift of 0.13%. A notable large horizontal crack appeared along the lapping region of south elevation followed by spalling of plaster within the story-drift of 0.2%. A vertical crack also appeared at the same position of existing shrinkage crack. Only minor cracks were seen in the north elevation. In the next stage of loading within the story-drift of 0.4%, the horizontal crack near loading point initiated in both in-plane walls. The horizontal crack elongated followed by appearance of a new vertical crack below the door of south elevation when story-drift was up to 0.67%. Within this drift, delamination of mesh was also observed at an elevation where the load was applied. The extension of previous crack continued with propagation in crack width at next stage of loading within the story-drift of 1.0%. Some plaster fell off at the top part of south elevation wall. At the final stage, the loading was applied until the story-drift was 1.33%. In this stage, numerous shear cracks were visible in north elevation, and in the south elevation there was spalling of plaster exposing the mesh inside.

The mesh-wrap retrofitting technique was found compatible with the rammed earth walls with minimal delamination in the loading area. The proposed retrofitting method was effective in controlling the crack appearance in the specimens wherein the cracks were uniformly distributed throughout the wall and prevented crack concentration in a specific wall region.

The cumulative base shears are also compared with the design base shear value computed with Eq. (1) as per the Indian Standard Code IS1893 [15].

$$V_b = A_h W_t \qquad (1)$$

Here, the design horizontal base shear coefficient, A_h is given by $(ZISa/g)/(2R)$, where Z is the zone factor taken as 0.36 for very severe seismic zone, I is the importance factor taken as 1 for a residential building, Sa/g is the spectral acceleration coefficient taken as 2.5 for a natural time period of approximately 0.2 seconds for a two-storied masonry building, and R is the response reduction factor taken as 1.5 for an unreinforced load bearing masonry wall building [15]. The Eq. (1) gives the design base shear value of 399.91kN for the unreinforced building specimen, and it is represented in Fig.6 with a blue dashed line. It is observed that both the retrofitted buildings exceeded the design base shear value by 1.78 times for RE-R-SHORT and 2.51 times in case of RE-R-LONG.
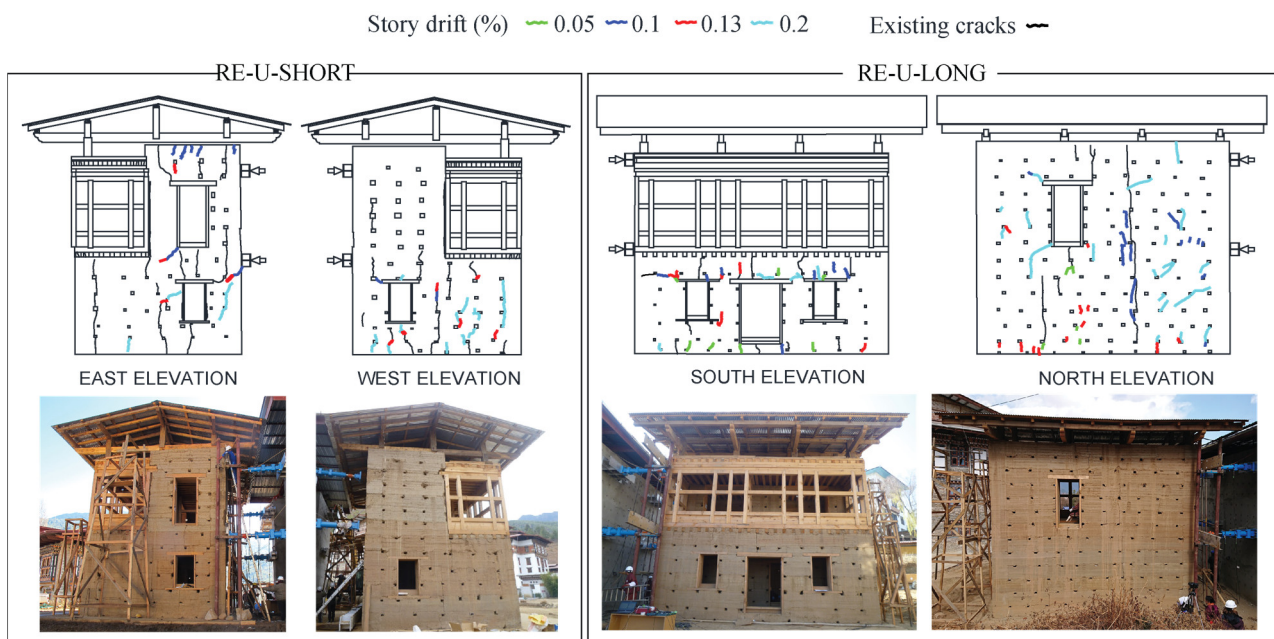

Fig. 8 – Crack patterns observed in unreinforced buildings: (RE-U-SHORT) and (RE-U-LONG)

8

Story drift (%) — 0.1 — 0.13 — 0.2 — 0.4 — 0.67 — 1 — 1.33

RE-R-SHORT

RE-R-LONG

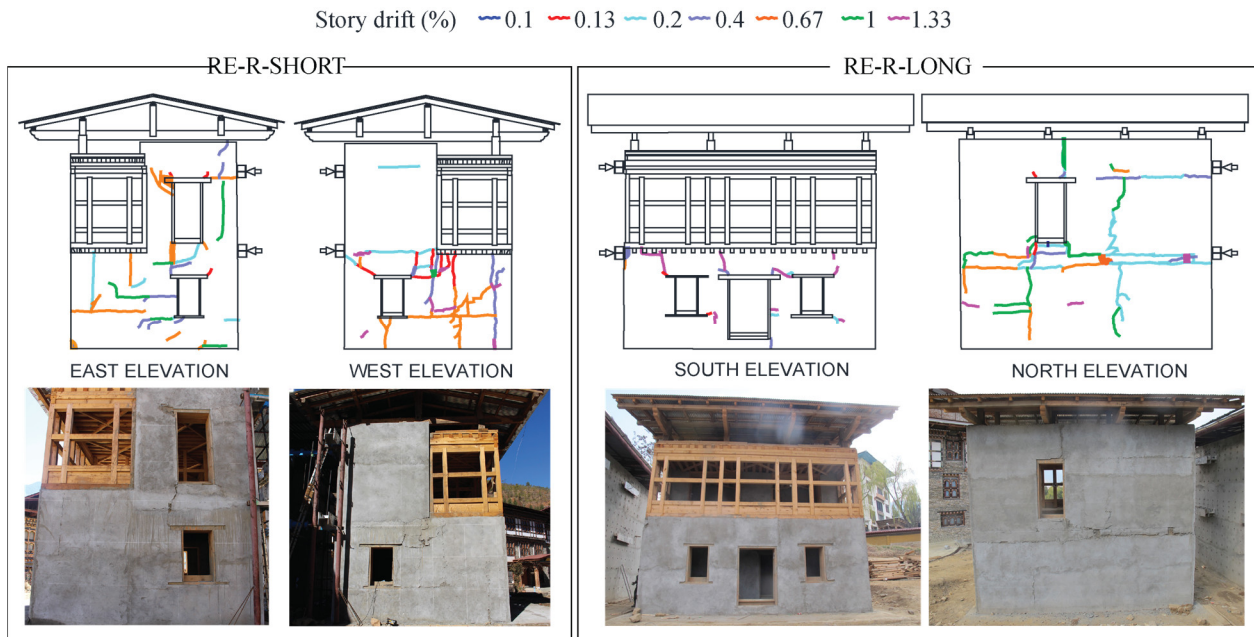EAST ELEVATION   WEST ELEVATION   SOUTH ELEVATION   NORTH ELEVATION

Fig. 9 – Crack patterns observed for retrofitted buildings: (RE-R-SHORT) and (RE-R-LONG)

A comparative study was done to understand the building response at two different orientations towards the loading in terms of the building capacity (Fig. 10) and damages incurred during the loading. The retrofitted rammed earth building loaded in long-span (RE-R-LONG) had considerably higher strength than the retrofitted rammed earth building loaded in short-span (RE-R-SHORT). The strength of RE-R-LONG was 1.41 times the RE-R-SHORT. However, the strength of RE-U-LONG was almost the same as RE-U-SHORT. The marginal difference in their capacity was probably because the shrinkage crack formed during the drying period in RE-U-LONG was more prominent and wider, which could have compromised the capacity of the building. The building orientation towards the loading influenced its' response under the static loading. The building, when loaded in short-span was almost symmetrical in plan with respect to the loading direction. The in-plane walls (east and west elevation of RE-SHORT) have almost same mass distribution, and the crack observed in these elevations were also almost uniform with same intensity. However, the building was asymmetrical when loaded in long-span. There was variation in mass distribution between two in-plane walls and subsequently, the amount of damages incurred in two elevations varied. The south elevation with higher mass suffered larger amount of damages than the north elevation.
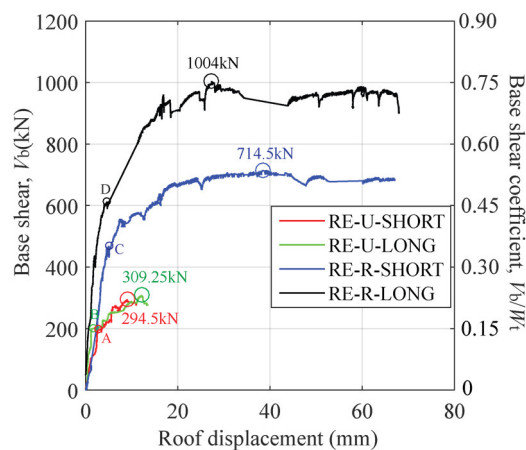
Fig. 10 – Capacity curve of all building specimens

9

3.2 Ductility and Energy absorption

The ductility index (μ) and energy absorption (Ψ) for each test specimens are listed in Table 2. The ductility here is defined as the ratio of the corresponding roof displacement at maximum base shear (Δ_{max}) to the displacement at yielding point (Δ_y). The yielding point here is considered to a point from the non-linear region right after the almost linear region of the capacity curve, where base shear imposed caused the appearance of the first crack in the building. The yielding points for each specimen are marked as A, B, C and D for RE-U-SHORT, RE-U-LONG, RE-R-SHORT and RE-R-LONG, respectively in Fig. 10. The ductility of both the retrofitted specimens is found higher than their unreinforced counterparts. It is evident from the capacity curve in Fig.11 that both retrofitted specimens have undergone substantial deformation without significant loss in the strength compared to the unreinforced specimens. The ductility of RE-R-SHORT was 2.22 times the RE-U-SHORT and RE-R-LONG was 1.38 times the RE-U-LONG. Comparing the ductility in terms of building orientation, the unreinforced building loaded in long-span (RE-U-LONG) exhibited better ductility than the unreinforced building loaded in short-span (RE-U-SHORT). However, after retrofitting them, the building loaded in short-span (RE-R-SHORT) had higher ductility than the building loaded in long-span (RE-R-LONG). The efficacy of mesh-wrap retrofitting technique was influenced by the orientation of the building towards the loading. The RE-R-SHORT in this orientation being in symmetrical to the loading was able to undergo larger deformation before it reached its maximum capacity.

Table 2 – Test results of full-scale static tests, ductility index and energy absorption for all specimens

Specimen Type	Base shear (kN)	Ψ (kN–mm)	Δ_{max} (mm)	Δ_y (mm)	μ (Δ_{max}/Δ_y)
RE-U-SHORT	294.5	1813.6	8.99	2.59	3.47
RE-R-SHORT	714.5	22679	38.48	4.99	7.71
RE-U-LONG	309.25	2852.5	12.16	2.48	4.90
RE-R-LONG	1004.0	21339	27.33	4.04	6.76

The energy absorption (Ψ) is given by the area under the maximum base shear and the corresponding top story–displacement curve. Both RE-R-SHORT and RE-R-LONG showed significantly higher energy absorption than RE-U-SHORT and RE-U-LONG, respectively. The retrofitted specimens could dissipate larger input energy compared to the unreinforced counterparts. The energy absorption values for RE-R-SHORT was 12.5 times the RE-U-SHORT and RE-R-LONG was 7.48 times the RE-U-LONG. For the unreinforced building, the energy absorption was observed higher for the building loaded in long-span (RE-U-LONG) compared to the building loaded in short-span (RE-U-SHORT). In case of the retrofitted buildings, the building loaded in short-span (RE-R-SHORT) which is symmetrical in this orientation towards the loading had higher energy absorption than the building loaded in long-span (RE-R-LONG).

4. Conclusions

The current study investigates the effect of building orientation in response to static loading while examining the efficacy of mesh-wrap retrofitting technique to enhance the strength of Bhutanese rammed earth buildings. Two full-scale unreinforced buildings were constructed representing the traditional Bhutanese buildings without any seismic resilient features. The study involved two phases of testing, the first phase involved full-scale test on unreinforced rammed earth buildings loaded in short-span and long-span, second phase involved full-scale test on the same set of buildings after retrofitting with the proposed technique. From the experimental test results, it was observed that mesh-wrap retrofitting had enhanced the capacity of rammed earth building by 2.43 times and 3.25 times for RE-SHORT and RE-LONG, respectively. The proposed retrofitting technique was found effective in improving the energy absorption and ductility index where the buildings underwent

10

larger deformation without a considerable decrease in the strength. The mesh-wrap retrofitting technique has enhanced the energy absorption by 12.5 times for RE-SHORT and 7.48 times for RE-LONG. The ductility index was also improved by 2.22 times and 1.38 times for RE-SHORT and RE-LONG, respectively by the proposed retrofitting technique. A study was also done to investigate the effect of building orientation towards loading to understand their behavior under static loading. The analysis has shown that the building loaded in long-span (RE-LONG) had had better strength compared to the building loaded in short-span (RE-SHORT). The building response under static loading was influenced by the building's orientation to the loading. The building with symmetrical in plan had uniform crack distribution in in-plane walls while the asymmetry building suffered more damages in elevation with higher mass. Based on the experimental results in this study and considering the retrofitting technique is simple, affordable, time-efficient and compatible with rammed earth walls, the mesh-wrap retrofitting method is recommended for the rammed earth buildings. Nevertheless, cement-based mortars have proven inadequate for unstabilised earth building plastering, due to their non-hygroscopic behavior, inhibiting needed walls water vapor exchange, as due to different mechanical and chemical properties [16,17] and are most likely to cause severe damages to rammed earth walls over time. Detachment among both wall and cement-based plaster usually occurs, while moisture-related wall degradation, earth grains cohesion loss, tends even to mine walls integrity. Further research therefore is suggested, in testing alternative hygroscopic material for plaster mortars, both suitable to earth walls technologies and granting experimented meshes efficiency.

5. Acknowledgements

6. References

[1] Miyamoto M, Aoki T, Tominaga Y, Pema (2014): Pull-down test of rammed earth walls at Paga Lhakhang in the Kingdom of Bhutan. *International Journal of Sustanaible Construction*, **2**, 51-59.

[2] Liu K, Wang M, Wang Y (2015): Seismic retrofitting of rural rammed earth buildings using externally bonded fibers. *Construction and Building Materials*, **100**, 91–101.

[3] Wang Y, Wang M, Liu K, Pan W, Yang X (2016): Shaking table tests on seismic retrofitting of rammed–earth structures. *Bulletin of Earthquake Engineering,* **15,** 1037–1055.

[4] Reyes JC, Rincon R, Yamin LE, Cprreal JF, Martinez JG, Sandoval JD, Gonzalez CD, Angel CC (2019): Seismic retrofitting of existing earthen structures using steel plates. *Construction and Building Materials*, **230**, 117039.

[5] Shrestha KC, Aoki T, Miyamoto M, Wangmo P, Pema, Zhang J, Takahashi N (2020): Strengthening of rammed earth structures with simple interventions. *Journal of Building Enginerring*, **29**, 101179.

[6] DCHS (2011): Damage Assesment of Rammed Earth Building-After the September 18, 2011 Earthqauke, Division for Conservation of Heritage Sites, Department of Culture, Ministry of Home and Cultual Affairs, Royal Government of Bhutan, Thimphu.

[7] Cheah JS, Morgan TKKB, Ingham and JM (2008): Cyclic testing of a full–size stablized, flax–fibre reinforced earth (Uku) wall system with openings. *The 14th World Conference on Earthquake Engineering*, Beijing, China.

[8] Miccoli L, Müller U, Pospíšil S (2017): Rammed earth walls strengthened with polyester fabric strips: Experimental analysis under in–plane cyclic loading. *Construction and Building Materials,* **149**, 29–36.

11

[9]   Fagone M, Loccarini F, Ranocchiai G (2017): Strength evaluation of jute fabric for the reinforcement of rammed earth structures. *Composites Part B: Engineering,* **113**, 1–13.

[10]   Pang M, Yang S, Zhang Y (2012); Experimental study of cement mortar–steel fiber reinforced rammed earth wall. *Sustainability*, **4**, 2630–2638.

[11]   Wangmo P, Shrestha KC, Miyamoto M, Aoki T (2018): Assessment of out of plane behaviour of rammed earth walls by pull-down tests. *International Journal of Architectural Heritage*, **13**, 273-287.

[12]   Shrestha KC, Aoki T, Konishi T, Miyamoto M, Zhang J, Takahashi N, Wangmo P, Aramaki T, Yuasa N (2019): Full-scale Pull-down tests on a two-storied rammed earth building with possible strengthening interventions. *Structural Analysis of Historical Construction*, **18**, 1557-1565.

[13]   ASTM C39/C39M–17b (2017): Standard test method for compressive strength of cylindrical concrete specimens. ASTM International, West Conshohocken, PA.

[14]   ASTM C496/C496–17 (2017): Standard test method for splitting tensile strength of cylindrical concrete 436 specimens, ASTM International, West Conshohocken, PA.

[15]   Indian Standard 1893 (Part 1): 2002 Indian Standard Criteria for earth resistant design of structures Part 1 General provisions and buildings, 5th edition, Bureau of Indian Standards, New Delhi.

[16]   Gomes MI, Faria P, Gonçalves TD (2018): Earth-based mortars for repair and protection of rammed earth walls. Stabilization with mineral binders and fibers. *Journal of Cleaner Production,* **172**, 2401-2414. Elsevier.

[17]   Boussalh M, Jlok M, Guillaud H, Moriset S (2004) : *Manuel de Conservation du Patrimoine Architectural en Terre des Valles Presahariennes du Maroc*. CERKAS-Centre du Patrimoine Mondial de l'UNESCO-CRATerre - Centre de Recherche et d'Application.

12